Research Article | Vol. 24, No. 23 | 14 Nov 2016 | OPTICS EXPRESS 25995

Optics EXPRESS

Experimental and numerical studies of the scattering of light from a two-dimensional randomly rough interface in the presence of total internal reflection: optical Yoneda peaks

ALMA K. GONZÁLEZ-ALCALDE,[1] JEAN-PHILIPPE BANON,[2] ØYVIND S. HETLAND,[2] ALEXEI A. MARADUDIN,[3] EUGENIO R. MÉNDEZ,[1] TOR NORDAM,[2] AND INGVE SIMONSEN[2,4,*]

[1] *División de Física Aplicada, Centro de Investigación Científica y de Educación Superior de Ensenada, Carretera Ensenada-Tijuana No. 3918, Ensenada B.C., 22860, México*
[2] *Department of Physics, NTNU Norwegian University of Science and Technology, NO-7491 Trondheim, Norway*
[3] *Department of Physics and Astronomy, University of California, Irvine, CA 92697, USA*
[4] *Surface du Verre et Interfaces, UMR 125 CNRS/Saint-Gobain, F-93303 Aubervilliers, France*
[*] *ingve.simonsen@ntnu.no*

Abstract: The scattering of polarized light from a dielectric film sandwiched between two different semi-infinite dielectric media is studied experimentally and theoretically. The illuminated interface is planar, while the back interface is a two-dimensional randomly rough interface. We consider here only the case in which the medium of incidence is optically more dense than the substrate, in which case effects due to the presence of a critical angle for total internal reflection occur. A reduced Rayleigh equation for the scattering amplitudes is solved by a rigorous, purely numerical, nonperturbative approach. The solutions are used to calculate the reflectivity of the structure and the mean differential reflection coefficient. Optical analogues of Yoneda peaks are present in the results obtained. The computational results are compared with experimental data for the in-plane mean differential reflection coefficient, and good agreement between theory and experiment is found.

OCIS codes: (240.0240) Optics at surfaces; (290.5880) Scattering, rough surfaces; (260.6970) Total internal reflection.

References and links

1. J. Nakayama, H. Ogura, and B. Matsumoto, "A probabilistic theory of scattering from a random rough surface," Radio Sci. **15**, 1049–1057 (1980).
2. T. Kawanishi, H. Ogura, and Z. L. Wang, "Scattering of an electromagnetic wave from a slightly random dielectric surface: Yoneda peak and Brewster angle in incoherent scattering," Wave. Random Media **7**, 351–384 (1997).
3. Y. Yoneda, "Anomalous Surface Reflection of X Rays," Phys. Rev. **131**, 2010–2013 (1963).
4. A. Soubret, G. Berginc, and C. Bourrely, "Application of reduced Rayleigh equations to electromagnetic wave scattering by two-dimensional randomly rough surfaces," Phys. Rev. B **63**, 245411 (2001).
5. T. Nordam, P. A. Letnes, and I. Simonsen, "Numerical simulations of scattering of light from two-dimensional rough surfaces using the reduced Rayleigh equation," Front. Phys. **1**, 8 (2013).
6. Ø. S. Hetland, A. A. Maradudin, T. Nordam, and I. Simonsen, "Numerical studies of the scattering of light from a two-dimensional randomly rough interface between two dielectric media," Phys. Rev. A **93**, 053819 (2016).
7. E. R. Méndez, G. D. Jiménez, and A. A. Maradudin, "A simple model of a one-dimensional, randomly rough, non-Gaussian surface," Proc. SPIE **9961**, 99610D (2016).
8. P. F. Gray, "A method of forming optical diffusers of simple known statistical properties," Opt. Acta **25**, 765–775 (1978).
9. B. E. Warren and J. S. Clarke, "Interpretation of the Anomalous Surface Reflection of X Rays," J. Appl. Phys. **36**, 324–325 (1965).
10. G. H. Vineyard, "Grazing-incidence diffraction and the distorted-wave approximation for the study of surfaces," Phys. Rev. B **26**, 4146–4159 (1982).
11. S. K. Sinha, E. B. Sirota, S. Garoff, and H. B. Stanley, "X-ray and neutron scattering from rough surfaces," Phys. Rev. B **38**, 2297–2311 (1988).
12. For reasons of convenience, a negative value of the polar angle of scattering, θ_s, is used to denote the case $\hat{\mathbf{q}}_{||} = -\hat{\mathbf{k}}_{||}$.

#272997 http://dx.doi.org/10.1364/OE.24.025995
Journal © 2016 Received 18 Aug 2016; revised 15 Oct 2016; accepted 16 Oct 2016; published 1 Nov 2016

Optics EXPRESS

1. Introduction

In many theoretical and experimental studies of the scattering of light from randomly rough surfaces the medium of incidence is vacuum. In the case that the scattering medium is a dielectric, this choice for the medium of incidence rules out investigations of interesting single- and multiple-scattering effects associated with the phenomenon of total internal reflection, which occurs when the medium of incidence is optically more dense than the scattering medium.

By use of the stochastic functional approach [1] Kawanishi *et al*. studied the coherent and incoherent scattering of an electromagnetic wave from a two-dimensional interface separating two different dielectric media [2]. The medium of incidence could be either medium. The theoretical approach used in this work was perturbative, and applicable only to weakly rough interfaces. Nevertheless it yielded interesting results, including the presence of Yoneda peaks in the angular dependence of the intensity of the light scattered back into the medium of incidence, when the latter is the optically more dense medium. These are sharp asymmetric peaks occurring at the critical angle for total internal reflection, for a fixed angle of incidence, for either p- or s-polarization of the incident light. These peaks were first observed experimentally in the scattering of x-rays incident from air on a metal surface [3]. Until now they have not been observed in optical experiments.

In subsequent work Soubret *et al*. [4] derived a reduced Rayleigh equation for the scattering amplitudes when an electromagnetic wave is incident from one dielectric medium on its two-dimensional randomly rough interface with a second dielectric medium. They obtained a solution of this equation as an expansion in powers of the surface profile through terms of third order, but in obtaining the numerical results presented in the paper the medium of incidence was assumed to be vacuum.

In this paper we remove two limitations present in earlier studies of the scattering of light from dielectric structures possessing one two-dimensional interface. The first constraint we remove is the lack of experimental results for scattering from two-dimensional randomly rough interfaces in the presence of total internal reflection. We present experimental results for the contribution to the mean differential reflection coefficient (DRC) from in-plane co-polarized scattering. These are the first experimental studies of such scattering, and they demonstrate the existence of Yoneda peaks at optical frequencies.

The second limitation we remove is the absence of nonperturbative solutions of the equations of scattering theory. We solve a reduced Rayleigh equation for the scattering amplitudes for the dielectric structure studied experimentally, by a rigorous, purely numerical, nonperturbative approach. The solutions are used to calculate the reflectivity and the mean DRC of the structure, the latter of which is compared with the experimental results.

2. Theoretical formulation

The scattering system we consider consists of a dielectric medium whose dielectric constant is ε_1 in the region $x_3 > 0$, a dielectric medium whose dielectric constant is ε_2 in the region $-d + \zeta(\mathbf{x}_\parallel) < x_3 < 0$, where $\mathbf{x}_\parallel = (x_1, x_2, 0)$, and a dielectric medium whose dielectric constant is ε_3 in the region $x_3 < -d + \zeta(\mathbf{x}_\parallel)$ [see Fig. 1]. The dielectric constants ε_1, ε_2, and ε_3 are all real and positive. The surface profile function $\zeta(\mathbf{x}_\parallel)$ is assumed to be a single-valued function of $\mathbf{x}_\parallel$ that is differentiable with respect to x_1 and x_2, and constitutes a stationary, zero-mean, isotropic, Gaussian random process. This random process is defined by the surface height autocorrelation function $\langle \zeta(\mathbf{x}_\parallel)\zeta(\mathbf{x}'_\parallel)\rangle = \delta^2 W(|\mathbf{x}_\parallel - \mathbf{x}'_\parallel|)$. The angle brackets here and in all that follows denote an average over the ensemble of realizations of the surface profile function, and $\delta = \langle \zeta^2(\mathbf{x}_\parallel)\rangle^{\frac{1}{2}}$ is the rms height of the surface.

Optics EXPRESS

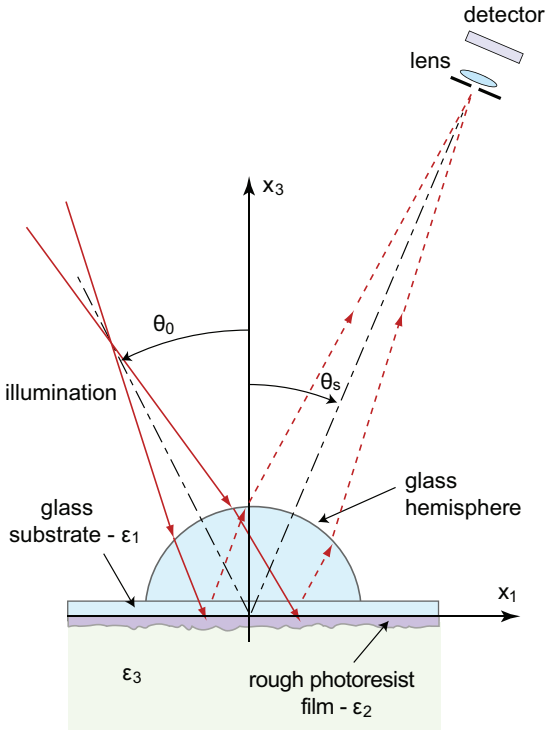

Fig. 1. Schematic diagram of the sample geometry.

We have chosen to study this structure instead of the simpler system of a single two-dimensional randomly rough interface separating two different dielectric media because it is the one employed in the experimental work whose results will be compared with the results of our calculations.

The interface $x_3 = 0$ is illuminated from the region $x_3 > 0$ by a plane wave of angular frequency ω. We write the electric field in this region as the sum of an incident field and a scattered field, $\mathbf{E}(\mathbf{x};t) = [\mathbf{E}(\mathbf{x}|\omega)_{\rm inc} + \mathbf{E}(\mathbf{x}|\omega)_{\rm sc}]\exp(-{\rm i}\omega t)$, where

$$\mathbf{E}(\mathbf{x}|\omega)_{\rm inc} = \left[\hat{\mathbf{e}}_p^{(i)}(\mathbf{k}_\parallel)E_{0p}(\mathbf{k}_\parallel) + \hat{\mathbf{e}}_s^{(i)}(\mathbf{k}_\parallel)E_{0s}(\mathbf{k}_\parallel)\right]\exp\left[{\rm i}\mathbf{k}_\parallel\cdot\mathbf{x}_\parallel - {\rm i}\alpha_1(k_\parallel)x_3\right] \tag{1a}$$

$$\mathbf{E}(\mathbf{x}|\omega)_{\rm sc} = \int \frac{{\rm d}^2q_\parallel}{(2\pi)^2}\left[\hat{\mathbf{e}}_p^{(s)}(\mathbf{q}_\parallel)A_p(\mathbf{q}_\parallel) + \hat{\mathbf{e}}_s^{(s)}(\mathbf{q}_\parallel)A_s(\mathbf{q}_\parallel)\right]\exp\left[{\rm i}\mathbf{q}_\parallel\cdot\mathbf{x}_\parallel + {\rm i}\alpha_1(q_\parallel)x_3\right], \tag{1b}$$

where $\alpha_i(q_\parallel) = [\varepsilon_i(\omega/c)^2 - q_\parallel^2]^{\frac{1}{2}}$ $(i = 1, 2, 3)$, with ${\rm Re}\,\alpha_i(q_\parallel) > 0$, ${\rm Im}\,\alpha_i(q_\parallel) > 0$, while

$$\hat{\mathbf{e}}_p^{(i)}(\mathbf{k}_\parallel) = \frac{\hat{\mathbf{k}}_\parallel\alpha_1(k_\parallel) + \hat{\mathbf{x}}_3 k_\parallel}{\sqrt{\varepsilon_1}\frac{\omega}{c}} \tag{2a}$$

$$\hat{\mathbf{e}}_s^{(i)}(\mathbf{k}_\parallel) = \hat{\mathbf{k}}_\parallel \times \hat{\mathbf{x}}_3 \tag{2b}$$

and

$$\hat{\mathbf{e}}_p^{(s)}(\mathbf{q}_\parallel) = \frac{-\hat{\mathbf{q}}_\parallel\alpha_1(q_\parallel) + \hat{\mathbf{x}}_3 q_\parallel}{\sqrt{\varepsilon_1}\frac{\omega}{c}} \tag{3a}$$

$$\hat{\mathbf{e}}_s^{(s)}(\mathbf{q}_\parallel) = \hat{\mathbf{q}}_\parallel \times \hat{\mathbf{x}}_3. \tag{3b}$$

Optics EXPRESS

A caret over a vector indicates that it is a unit vector. In Eq. (1) $E_{0p}(\mathbf{k}_\parallel)$ and $E_{0s}(\mathbf{k}_\parallel)$ are the amplitudes of the p- and s-polarized components of the incident field with respect to the plane of incidence, defined by the vectors $\hat{\mathbf{k}}_\parallel$ and $\hat{\mathbf{x}}_3$. Similarly, $A_p(\mathbf{q}_\parallel)$ and $A_s(\mathbf{q}_\parallel)$ are the amplitudes of the p- and s-polarized components of the scattered field with respect to the plane of scattering, defined by the vectors $\hat{\mathbf{q}}_\parallel$ and $\hat{\mathbf{x}}_3$.

Maxwell's equations and the associated boundary conditions at the interfaces $x_3 = 0$ and $x_3 = -d + \zeta(\mathbf{x}_\parallel)$ imply a linear relation between $A_p(\mathbf{q}_\parallel)$, $A_s(\mathbf{q}_\parallel)$ and $E_{0p}(\mathbf{k}_\parallel)$, $E_{0s}(\mathbf{k}_\parallel)$, which we write as ($\alpha = p, s$, $\beta = p, s$)

$$A_\alpha(\mathbf{q}_\parallel) = \sum_\beta R_{\alpha\beta}(\mathbf{q}_\parallel|\mathbf{k}_\parallel) E_{0\beta}(\mathbf{k}_\parallel). \tag{4}$$

The equations satisfied by the scattering amplitudes $\{R_{\alpha\beta}(\mathbf{q}_\parallel|\mathbf{k}_\parallel)\}$ can be written in the form

$$\int \frac{\mathrm{d}^2 q_\parallel}{(2\pi)^2} \mathbf{M}^+(\mathbf{p}_\parallel|\mathbf{q}_\parallel)\mathbf{R}(\mathbf{q}_\parallel|\mathbf{k}_\parallel) = -\mathbf{M}^-(\mathbf{p}_\parallel|\mathbf{k}_\parallel), \tag{5}$$

where

$$\mathbf{R}(\mathbf{q}_\parallel|\mathbf{k}_\parallel) = \begin{pmatrix} R_{pp}(\mathbf{q}_\parallel|\mathbf{k}_\parallel) & R_{ps}(\mathbf{q}_\parallel|\mathbf{k}_\parallel) \\ R_{sp}(\mathbf{q}_\parallel|\mathbf{k}_\parallel) & R_{ss}(\mathbf{q}_\parallel|\mathbf{k}_\parallel) \end{pmatrix} \tag{6}$$

$$\mathbf{M}^\pm(\mathbf{p}_\parallel|\mathbf{q}_\parallel) = \begin{pmatrix} M^\pm_{pp}(\mathbf{p}_\parallel|\mathbf{q}_\parallel) & M^\pm_{ps}(\mathbf{p}_\parallel|\mathbf{q}_\parallel) \\ M^\pm_{sp}(\mathbf{p}_\parallel|\mathbf{q}_\parallel) & M^\pm_{ss}(\mathbf{p}_\parallel|\mathbf{q}_\parallel) \end{pmatrix}, \tag{7}$$

and the matrix elements are expressed as [4]

$$\begin{aligned}\mathbf{M}^\pm_{pp}(\mathbf{p}_\parallel|\mathbf{q}_\parallel) =& \frac{1}{\alpha_2(q_\parallel)}\Big\{ I_-(\mathbf{p}_\parallel|\mathbf{q}_\parallel)\left[p_\parallel q_\parallel + \alpha_3(p_\parallel)\hat{\mathbf{p}}_\parallel\cdot\hat{\mathbf{q}}_\parallel\alpha_2(q_\parallel)\right]\left[\varepsilon_1\alpha_2(q_\parallel) \pm \varepsilon_2\alpha_1(q_\parallel)\right] \\ &+ I_+(\mathbf{p}_\parallel|\mathbf{q}_\parallel)\left[p_\parallel q_\parallel - \alpha_3(p_\parallel)\hat{\mathbf{p}}_\parallel\cdot\hat{\mathbf{q}}_\parallel\alpha_2(q_\parallel)\right]\left[\varepsilon_1\alpha_2(q_\parallel) \mp \varepsilon_2\alpha_1(q_\parallel)\right]\Big\} \end{aligned} \tag{8a}$$

$$\begin{aligned}\mathbf{M}^\pm_{sp}(\mathbf{p}_\parallel|\mathbf{q}_\parallel) =& \sqrt{\varepsilon_3}\frac{\omega}{c}\left[\hat{\mathbf{p}}_\parallel\times\hat{\mathbf{q}}_\parallel\right]_3 \\ &\times\Big\{ I_-(\mathbf{p}_\parallel|\mathbf{q}_\parallel)\left[\varepsilon_1\alpha_2(q_\parallel) \pm \varepsilon_2\alpha_1(q_\parallel)\right] - I_+(\mathbf{p}_\parallel|\mathbf{q}_\parallel)\left[\varepsilon_1\alpha_2(q_\parallel) \mp \varepsilon_2\alpha_1(q_\parallel)\right]\Big\} \end{aligned} \tag{8b}$$

$$\begin{aligned}\mathbf{M}^\pm_{ps}(\mathbf{p}_\parallel|\mathbf{q}_\parallel) =& -\sqrt{\varepsilon_1}\varepsilon_2\frac{\omega}{c}\left[\hat{\mathbf{p}}_\parallel\times\hat{\mathbf{q}}_\parallel\right]_3\frac{\alpha_3(p_\parallel)}{\alpha_2(q_\parallel)} \\ &\times\Big\{ I_-(\mathbf{p}_\parallel|\mathbf{q}_\parallel)\left[\alpha_2(q_\parallel) \pm \alpha_1(q_\parallel)\right] + I_+(\mathbf{p}_\parallel|\mathbf{q}_\parallel)\left[\alpha_2(q_\parallel) \mp \alpha_1(q_\parallel)\right]\Big\} \end{aligned} \tag{8c}$$

$$\begin{aligned}\mathbf{M}^\pm_{ss}(\mathbf{p}_\parallel|\mathbf{q}_\parallel) =& \sqrt{\varepsilon_1}\varepsilon_2\sqrt{\varepsilon_3}\left(\frac{\omega}{c}\right)^2\hat{\mathbf{p}}_\parallel\cdot\hat{\mathbf{q}}_\parallel\frac{1}{\alpha_2(q_\parallel)} \\ &\times\Big\{ I_-(\mathbf{p}_\parallel|\mathbf{q}_\parallel)\left[\alpha_2(q_\parallel) \pm \alpha_1(q_\parallel)\right] + I_+(\mathbf{p}_\parallel|\mathbf{q}_\parallel)\left[\alpha_2(q_\parallel) \mp \alpha_1(q_\parallel)\right]\Big\}. \end{aligned} \tag{8d}$$

In writing Eq. (8) we have defined

$$I_\pm(\mathbf{p}_\parallel|\mathbf{q}_\parallel) = \exp\{\mathrm{i}[\alpha_3(p_\parallel) \pm \alpha_2(q_\parallel)]d\}\frac{I(\alpha_3(p_\parallel) \pm \alpha_2(q_\parallel)|\mathbf{p}_\parallel - \mathbf{q}_\parallel)}{\alpha_3(p_\parallel) \pm \alpha_2(q_\parallel)}, \tag{9}$$

where d is the mean thickness of the film, and

$$I(\gamma|\mathbf{Q}_\parallel) = \int \mathrm{d}^2 x_\parallel \, \exp\left[-\mathrm{i}\gamma\zeta(\mathbf{x}_\parallel)\right]\exp\left(-\mathrm{i}\mathbf{Q}_\parallel\cdot\mathbf{x}_\parallel\right). \tag{10}$$

Optics EXPRESS

The contribution to the mean DRC from the light that has been scattered incoherently (diffusely), and the reflectivity of the scattering system can be expressed in terms of the scattering amplitudes $\{R_{\alpha\beta}(\mathbf{q}_\parallel|\mathbf{k}_\parallel)\}$. Thus, the fraction of the total time-averaged flux in an incident wave of polarization β, the projection of whose wave vector on the mean scattering plane is $\mathbf{k}_\parallel$ that is scattered incoherently into a wave of α polarization, the projection of whose wave vector on the mean scattering plane is $\mathbf{q}_\parallel$, within an element of solid angle $\mathrm{d}\Omega_s$ about the scattering direction defined by the polar and azimuthal scattering angles (θ_s, ϕ_s), is given by

$$\left\langle \frac{\partial R_{\alpha\beta}(\mathbf{q}_\parallel|\mathbf{k}_\parallel)}{\partial\Omega_s} \right\rangle_{\text{incoh}} = \frac{\varepsilon_1}{S}\left(\frac{\omega}{2\pi c}\right)^2 \frac{\cos^2\theta_s}{\cos\theta_0}\left[\langle|R_{\alpha\beta}(\mathbf{q}_\parallel|\mathbf{k}_\parallel)|^2\rangle - |\langle R_{\alpha\beta}(\mathbf{q}_\parallel|\mathbf{k}_\parallel)\rangle|^2\right]. \tag{11}$$

Here S is the area of the plane $x_3 = 0$ covered by the random surface, and we have used the relations $\mathbf{k}_\parallel = \sqrt{\varepsilon_1}(\omega/c)\sin\theta_0(\cos\phi_0, \sin\phi_0, 0)$ and $\mathbf{q}_\parallel = \sqrt{\varepsilon_1}(\omega/c)\sin\theta_s(\cos\phi_s, \sin\phi_s, 0)$. Similarly, the reflectivity for light of polarization α incident on the surface with a polar angle of incidence θ_0 is

$$\mathcal{R}_\alpha(\theta_0) = \left|R_\alpha(k_\parallel)\right|^2 = \left|R_\alpha(\sqrt{\varepsilon_1}(\omega/c)\sin\theta_0)\right|^2, \tag{12}$$

where $R_\alpha(k_\parallel) = \langle R_{\alpha\alpha}(\mathbf{k}_\parallel|\mathbf{k}_\parallel)\rangle/S$.

The numerical solution of equations like Eq. (5) is described in detail in [5].

The theoretical results given by Eqs. (5)–(7) are valid both when the medium of incidence is optically more dense than the substrate and when it is optically less dense. However, in this paper we will present computational and experimental results only for the former case, because it is only in that case that effects due to total internal reflection occur. Results for the latter case will be presented elsewhere [6].

3. Experimental details

We have conducted angular scattering experiments with specially fabricated randomly rough surfaces. They were fabricated by exposing photoresist-coated plates (Shipley 1805) to statistically independent speckle patterns [8]. The speckle patterns were produced by passing a He-Cd laser beam ($\lambda = 442\,\text{nm}$) through a ground glass plate. The samples consist then of a glass substrate ($\varepsilon_1 = 2.25$), covered with a randomly rough film of photoresist ($\varepsilon_2 = 2.69$) in contact with air ($\varepsilon_3 = 1$), see Fig. 1.

Due to the exposure characteristics, the surfaces should have approximately Gaussian statistics and a Gaussian correlation function. They were characterized optically (by the strength of the coherent component) and by means of a mechanical profilometer. We present scattering data obtained from a surface whose rms height is $\delta = 22\,\text{nm}$ and its transverse correlation length $a = 1.9\,\mu\text{m}$. In the visible region of the spectrum, theories based on the reduced Rayleigh equation are adequate to deal with surfaces with such characteristic parameters. The mean film thickness of the sample is $d = 0.6\,\mu\text{m}$.

The experimental arrangement is shown in Fig. 1. The intensity was measured as a function of angle using a scatterometer that consists of an illumination and a detection system whose angular position can be controlled by a computer using two rotary stages with an angular resolution of 0.25 degrees. The illumination system consists of a HeNe laser beam ($\lambda = 632.8\,\text{nm}$) and a series of mirrors, diaphragms and lenses. The intensity and polarization of the illumination were controlled by placing, in series, a circular and a linear polarizer.

In order to illuminate the surface from the optically denser medium with angles of incidence close to the total internal reflection angle, the substrate was put in optical contact with a glass hemisphere (about 3.7 cm in diameter) using index matching oil [see Fig. 1]. A converging beam was focused a couple of centimeters before the glass hemisphere so that, after refraction at the hemisphere, the photoresist-air interface was illuminated by a diverging beam. The scattered

Optics EXPRESS

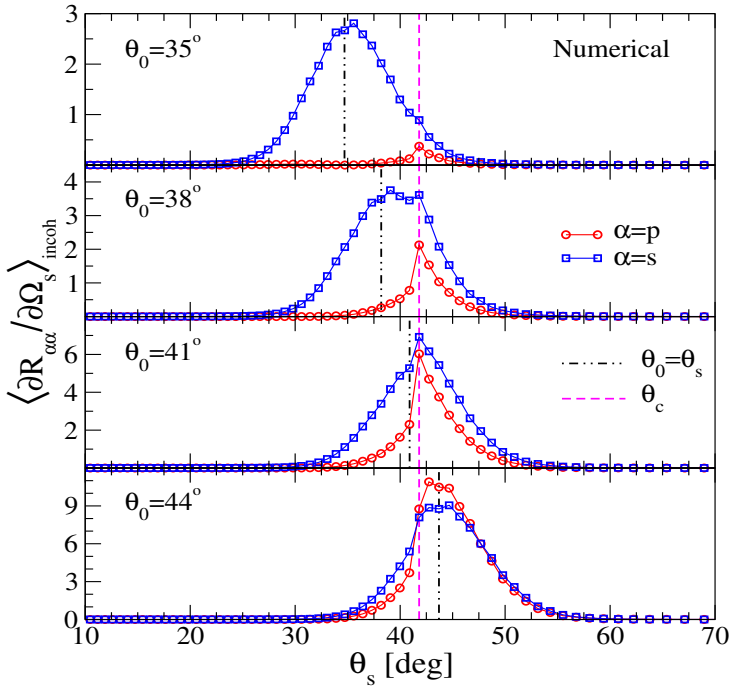

Fig. 2. The in-plane angular dependence of $\langle \partial R_{\alpha\alpha}/\partial\Omega_s \rangle_{\text{incoh}}$ for a set of θ_0 obtained by the numerical approach outlined in the text. The open symbols represents the data points obtained in the simulations, while the lines connecting them, are only included as a guide to the eye. Notice how the amplitudes of the data vary from panel to panel.

light passed again through the glass hemisphere and was collected by the detection system, about 30 cm away, in what is, effectively, the far field of the rough photoresist-air interface. The detection system consisted, basically, of a lens and a silicon detector. To reduce noise in the measurements, the detected signal was processed using lock-in detection techniques. For this, a mechanical chopper and a lock-in amplifier were used in the illumination and detection systems, respectively.

The use of the hemisphere permits the illumination of the rough interface with angles of incidence beyond the critical angle and simplifies the measurements of the angular distribution of scattered light. On the other hand, it introduces some experimental difficulties. First of all, the light has to pass twice through an interface with high optical power and, in a symmetric system (equal distances to the point source and to its image, obtained by specular reflection from the photoresist-air interface), the conjugate distances are practically equal to the diameter of the hemisphere. To facilitate the measurements, the first conjugate (source of the diverging beam) must be placed close to the hemisphere, so that the second conjugate point moves away from the sample, as shown in Fig. 1. The detection system moves then in a circle whose radius is determined by the position where the light that is specularly reflected by the rough photoresist-air interface is focused.

The alignment of the whole system is quite demanding. It is hard to make the center of curvature of the glass hemisphere coincide with the center of rotation of the sample, which makes it difficult to establish the angles of incidence and scattering with precision. However, since the critical angle is determined solely by the dielectric constants of the flat photoresist-air interface, this difficulty was circumvented by making the critical angle observed in the measurements coincide with the theoretical value of the critical angle. The other issue worth mentioning is

Optics EXPRESS

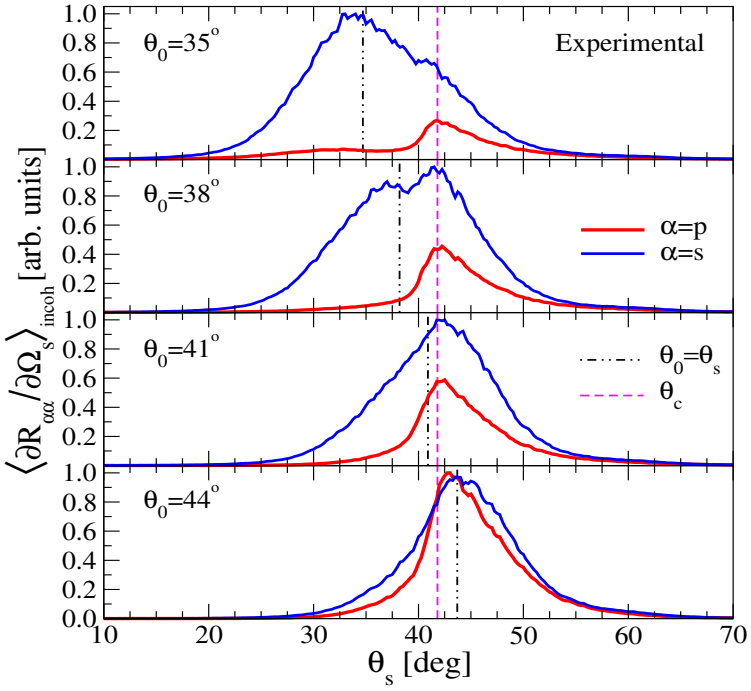

Fig. 3. Same as Fig. 2 but now presenting experimental measurements. The data sets in each panel were scaled by a common factor so that a unit amplitude corresponds to the maximum value of the corresponding numerical simulation results presented in Fig. 2.

that, since it is not possible to measure directly the light incident on the rough photoresist-air interface, it is difficult to obtain scattering data normalized by the incident power.

4. Results and discussion

Numerical and experimental results for the contribution to the mean DRC from in-plane co-polarized light scattered incoherently by the rough surface, $\langle \partial R_{\alpha\alpha}/\partial\Omega_s \rangle_{\text{incoh}}$, are presented in Figs. 2 and 3, respectively, for the same values of θ_0. By also calculating the transmitted intensity, energy conservation was found to be satisfied in our calculations with an error smaller than 10^{-3} (see [6] for details). For polar angles of incidence $\theta_0 \lesssim \theta_0^\star = 30°$, no pronounced Yoneda peaks are observed, either in the experimental or numerical data; at least, this is true for the structure that we considered. However, when the angle of incidence is increased towards the critical angle for total internal reflection $\theta_c = 41.89°$ [$\theta_0^\star \lesssim \theta_0 < \theta_c$], Yoneda peaks gradually start to develop around $\theta_s = \theta_c$ [Figs. 2 and 3; panels $\theta_0 = 35°, 38°$]. Initially these peaks are most readily observed in p-to-p scattering, but for an angle of incidence in the vicinity of the critical angle, $\theta_0 \lesssim \theta_c$, Yoneda peaks are also clearly identifiable in s-to-s scattering. Finally, for $\theta_0 > \theta_c$, Yoneda peaks are no longer observed either in the numerical or experimental data, and the signal amplitude at their position starts to drop off as one approaches grazing incidence [see Fig. 4].

There is a good quantitative agreement between the predicted angular positions of the Yoneda peaks presented in Fig. 2, and the experimental positions presented in Fig. 3. There is qualitative agreement about how these peaks develop with an increase of the polar angle of incidence. However, the experimental distributions $\langle \partial R_{\alpha\alpha}/\partial\Omega_s \rangle_{\text{incoh}}$ are broader then their numerical counterparts, and the ratio of the amplitudes of the two co-polarized experimental intensity distributions are not consistently reproduced by the numerical simulation results. We attribute

Optics EXPRESS

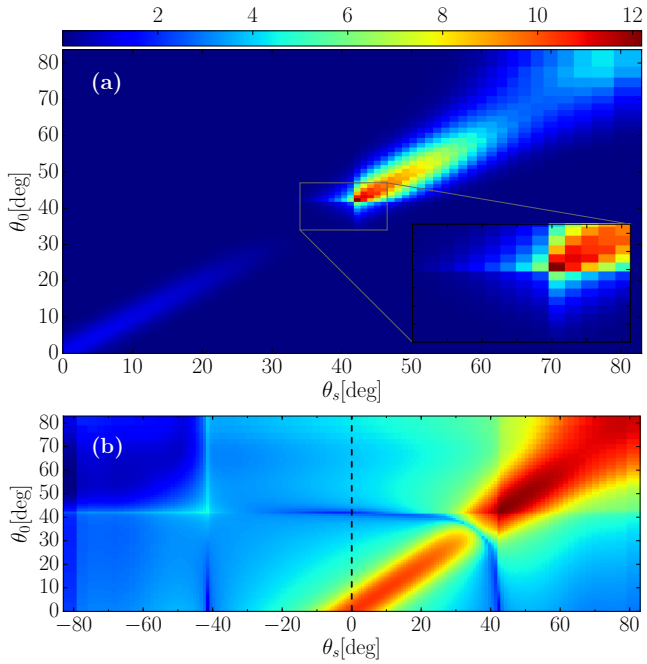

Fig. 4. Contour maps of the in-plane dependence of the raw simulation data for the co-polarized mean DRC as functions of θ_s and θ_0. Figure 4(a) represents the contour map of $\langle \partial R_{pp}/\partial \Omega_s \rangle_{\text{incoh}}$ and its inset details the behavior around $(\theta_s, \theta_0) = (\theta_c, \theta_c)$. In Fig. 4(b) the logarithm of the same data, $\log\langle \partial R_{pp}/\partial \Omega_s \rangle_{\text{incoh}}$, are presented but over the full range of polar scattering angles $-90° < \theta_s < 90°$. The vertical dashed center line (black) indicates $\theta_s = 0°$.

these differences between the experimental and numerical results in part to deviations of the statistical properties of the fabricated randomly rough surface used in the experiments from those assumed in performing the numerical calculations [7].

To better represent the dependence of the incoherently scattered light on the polar angles of incidence and scattering, in Fig. 4 we present contour maps of the angular dependence of the computational results for the in-plane, p-to-p incoherent scattering contribution to the mean DRC. The inset in Fig. 4(a) details the region around $(\theta_s, \theta_0) = (\theta_c, \theta_c)$ and explicitly shows the asymmetric character of the Yoneda peak phenomenon. To more readily inspect the local variations of this data set, Fig. 4(b) presents a contour plot of $\log\langle \partial R_{pp}/\partial \Omega_s \rangle_{\text{incoh}}$ as a function of θ_s and θ_0 for $-90° < \theta_s < 90°$ [12]. Several features of the scattered intensity should be noted from the results presented in Fig. 4(b). The first feature is the rapid intensity variations in the angular region around $\theta_0 = \theta_c$ or $\theta_s = \pm\theta_c$. For instance, at normal incidence [$\theta_0 = 0°$], local minima in the p-to-p scattered intensity distributions are observed around $\theta_s \approx \pm\theta_c$ [seen as the dark blue vertical structures in Fig. 4(b)]. As the polar angle of incidence is increased, the scattered intensity distribution is transformed from displaying local *minima* around $\theta_s \approx \pm\theta_c$ to displaying local *maxima* around the same angles. Only in the latter case does the scattered intensity distribution show Yoneda peaks, the phenomenon that we study experimentally in this work. It should be mentioned that in a recent numerical study of a related scattering system, a similar variation of the in-plane, p-to-p scattered intensity around $\theta_s \approx \pm\theta_c$ was observed and explained theoretically [6]. In this publication it was also shown that the in-plane, s-to-s scattered intensity displays Yoneda peaks independent of the value of the polar angle of incidence.

Optics EXPRESS

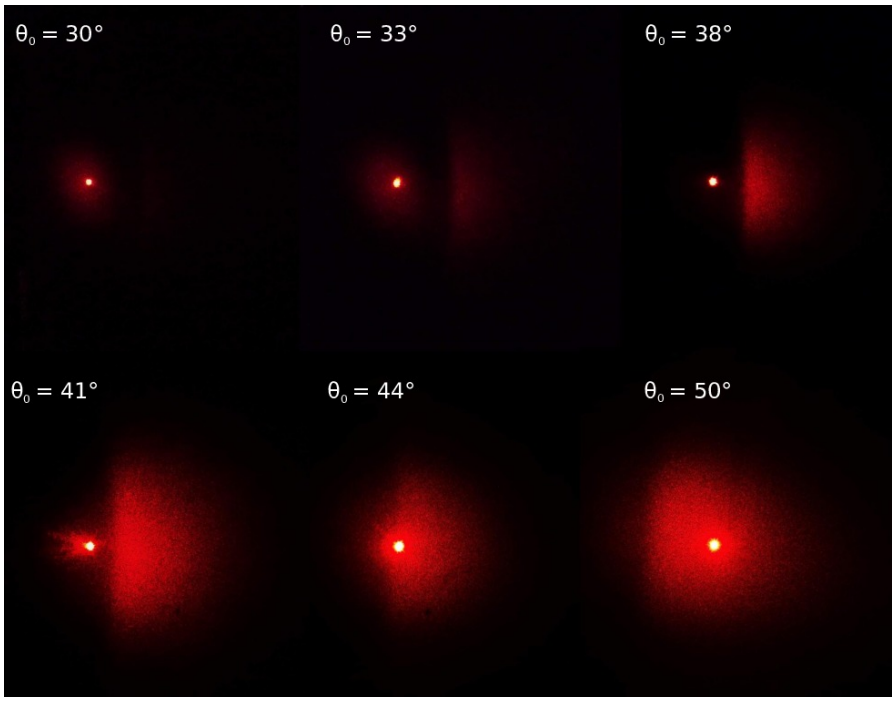

Fig. 5. Photographs showing the spatial intensity distributions formed on the rough aluminum screen [see Fig. 6] for a set of polar angles of incidence, $\theta_0 = \theta_s$, as indicated in the figure.

Figure 5 presents experimental results for the *angular dependence* of the intensity distributions of the light scattered also outside the plane of incidence; as such, these results complement the measured in-plane intensity distributions reported in Fig. 3.

The photographs of the scattered intensity patterns depicted in Fig. 5, were obtained with the arrangement illustrated in Fig. 6. As in the scattering measurements reported in Fig. 3, the sample is illuminated through a glass hemisphere, and the light is scattered back from the rough back surface of the sample through the glass hemisphere. However, in contrast to how the scattering measurements were preformed to produce the results of Fig. 3, a rough aluminum screen was placed about 45 cm from the sample so that the light would rescatter from it and form an image on the screen. A digital camera was then used to take photographs of the scattering patterns observed on the aluminum screen. It is in this way that the photographs shown in Fig. 5 were obtained.

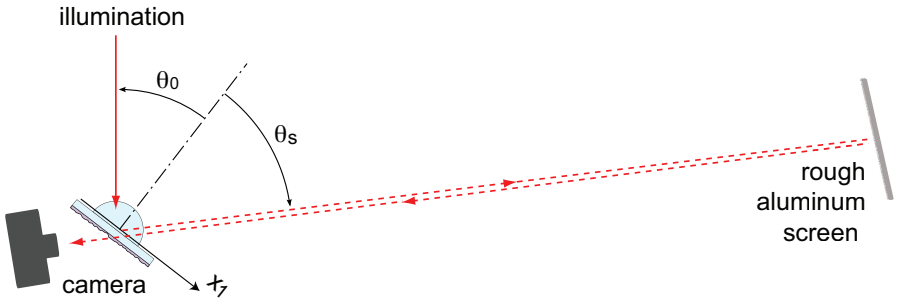

Fig. 6. Schematics of the geometry used to take the photographs presented in Fig. 5.

Optics EXPRESS

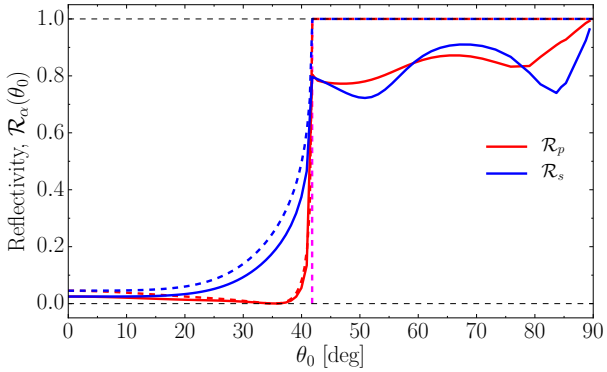

Fig. 7. The reflectivity, $\mathcal{R}_\alpha(\theta_0)$, of the scattering system studied. The dashed lines denotes the Fresnel reflection coefficient, *i.e.* the reflectivity of a corresponding film with planar surfaces.

The specular direction is represented by the bright red circular spots readily observed in the results presented in Fig. 5. As the polar angle of incidence is approaching the critical angle for total internal reflection $\theta_c = 41.89°$, the Yoneda peaks start to appear. In particular, for the intensity distributions presented in Fig. 5 corresponding to the polar angles of incidence 38° and 41°, the Yoneda phenomenon is clearly seen. It is manifested by an abrupt increase in the intensity of the scattered light in directions parallel to the plane of incidence. This results in a "ridge" of high intensity that locally is oriented almost perpendicular to the plane of incidence. This finding is consistent with the theoretical prediction for the full angular intensity distribution of the light scattered from a sample of similar geometry [6].

Although small amplitude perturbation theory predicts that the Yoneda peaks occur in the contribution to the scattering amplitudes $\{R_{\alpha\beta}(\mathbf{q}_\parallel|\mathbf{k}_\parallel)\}$ of first order in the surface profile function [6], and so are single-scattering phenomena, their physical interpretation has been the subject of discussion for five decades. In a study of the reflection of x-rays from a polished surface Warren and Clark [9] proposed that these peaks can be interpreted in terms of a small angle scattering from a projection on an irregular surface followed by total reflection. In a subsequent study of grazing-angle reflection of x-rays from rough metal surfaces, Vineyard [10] noted that the angular dependence of the Fresnel coefficient for transmission through a planar vacuum-metal interface produces a transmitted field on the surface whose angular dependence has the form of an asymmetric peak. The maximum of this peak occurs at the critical angle for total internal reflection and has a magnitude that is twice that of the incident electric field on the surface, which leads to an enhanced diffuse scattering at this angle. This effect was invoked by Sinha *et al.* [11] as the origin of the Yoneda peaks. However, it is not a physical explanation for the origin of these peaks. Kawanishi *et al.* [2] suggested that the Yoneda peaks may be due to the presence of lateral waves, excited through the roughness, propagating along the interface in the optically less dense medium. This wave satisfies the condition for refraction back into the optically more dense medium, and therefore leaks energy at each point along the interface along rays whose scattering angle equals θ_c. This explanation is attractive, but should be explored more through additional calculations.

Finally, in Fig. 7 we present the calculated reflectivity of our structure for p- and s-polarized incident light. The effect of total internal reflection is clearly seen in these results. For $\theta_c < \theta_0 < 90°$ the reflectivity in each polarization decreases by approximately 20% from the corresponding Fresnel reflectivity in much of this interval, a significant change for the degree of roughness possessed by this surface.

Optics EXPRESS

5. Conclusions

In this paper we have presented the first experimental results for the scattering of p- and s-polarized light from a dielectric structure with a two-dimensional randomly rough interface that can display effects associated with total internal reflection. In particular, we have shown the existence of Yoneda peaks in the angular dependence of the mean differential reflection coefficient. The experimental results are supported by the results of rigorous, purely numerical, nonperturbative solutions of the reduced Rayleigh equation for scattering from this structure. These features are already present in single-scattering calculations of the mean differential reflection coefficient. It will be of interest to see how they develop in the presence of strong multiple scattering and in transmission. Finally, we find that even a small degree of roughness significantly depresses the reflection of p- and s-polarized light for scattering angles greater than the critical angle for total internal reflection.

Funding

Consejo Nacional de Ciencia y Tecnología (CONACYT) (180654); The Research Council of Norway (RCN) (216699); The French National Research Agency (ANR) (ANR-15-CHIN-0003-01).

Acknowledgments

This research was supported in part by NTNU and the Norwegian metacenter for High Performance Computing (NOTUR) by the allocation of computer time.